Li et al. BMC Microbiology (2016) 16:222
DOI 10.1186/s12866-016-0842-0

BMC Microbiology

RESEARCH ARTICLE Open Access

Mycoplasma ovipneumoniae induces sheep airway epithelial cell apoptosis through an ERK signalling-mediated mitochondria pathway

Yanan Li[1,2], Zhongjia Jiang[1,2], Di Xue[1,2], Guangcun Deng[1,2], Min Li[1,2], Xiaoming Liu[1,2,3*] and Yujiong Wang[1,2*]

Abstract

Background: *Mycoplasma ovipneumoniae* (*M. ovipneumoniae*) is a species of Mycoplasma bacteria that specifically infects sheep and goat, causing ovine infectious pleuropneumonia. However, the mechanism underlying the pathogen-host interaction between *M. ovipneumoniae* and airway epithelial cells is unknown.

Methods: A primary air-liquid interface (ALI) epithelial culture model generated from the bronchial epithelial cells of Ningxia *Tan sheep* (*ovis aries*) was employed to explore the potential mechanism of *M. ovipneumoniae*-induced cell apoptosis by characterizing the production of reactive oxygen species (ROS), methane dicarboxylic aldehyde (MDA) and anti-oxidative enzymes, as well as the mitochondrial membrane potentials, cytochrome C release, and activities of ERK and caspase signalling pathways.

Results: Increased ROS production and MDA concentration with mitochondrial membrane dysfunction and apoptotic cell death but decreased expression of the antioxidant enzymes catalase (CAT), glutathione synthetase (GSS), total superoxide dismutaes (T-SOD) and Mn-SOD were observed in sheep airway epithelial cells infected with *M. ovipneumoniae*. Mechanistically, the *M. ovipneumoniae*-induced cell apoptosis and disruption of mitochondrial integrity reflected mechanisms by which pathogen-activated mitogen-activated protein kinase (MAPK) signalling sequentially led to mitochondrial damage and release of Cyt-C into the cytoplasm, which in turn triggered the activation of caspase signalling cascade, resulting in the apoptosis of host cells.

Conclusions: These results suggest that *M. ovipneumoniae*-induced ROS and MAPK signalling-mediated mitochondrial apoptotic pathways might play key roles in the pathogenesis of *M. ovipneumoniae* infection in sheep lungs.

Keywords: *M. ovipneumoniae*, Sheep, Airway epithelial cells, Apoptosis, Mitochondrial pathway

Background

Mycoplasma pneumonia (*M. ovipneumoniae*) is a species of mycoplasma bacteria that specifically infect both sheep (*Ovis aries*) and goats. Since these bacteria were first isolated from the lung tissue of sheep with lung adenoma in 1963 [1], the mechanisms underpinning its pathogenesis have been extensively investigated. Studies have been demonstrated that airway epithelial cells are the main targets of *M. ovipneumoniae* infections and that these cells play an important role in host-pathogen interactions and the pathogenesis of mycoplasma infections in the lung, beyond their roles as the first line of physical barriers in defending against microbial infections and environmental stresses [2, 3]. In this context, airway epithelial cells maintain local immune homeostasis by producing cytokines and mucoproteins [4]. In mycoplasma infections, the adhesion of the pathogens to airway epithelial cells is the first key step towards infection, through which mycoplasma bacteria gain the ability to escape from clearance host immune responses [5].

A compelling body of evidence suggests that the metabolic products of mycoplasma cells induce significant

* Correspondence: liuxiaoming@nxmu.edu.cn; wyj@nxu.edu.cn
[1]Key Laboratory of Ministry of Education for Conservation and Utilization of Special Biological Resources in the Western, Yinchuan, Ningxia 750021, China
Full list of author information is available at the end of the article

oxidative damage, cell pathological changes and apoptosis by producing a large amount of H_2O_2 after they adhered to host epithelial cells [6–12]. Under physiological conditions, the host cells can balance the metabolism of oxygen-free radicals through defence mechanisms [13]. However, under pathological circumstances, oxidative stress caused by excessive oxygen free-radicals might lead to cell injury by mechanisms involved in mitochondrial dysfunction [14, 15] and the reduction of activities of antioxidant enzymes, including superoxide dismutase (SOD) [16], catalase (CAT) [17, 18] and glutathione synthetase (GSS) [19, 20]. The increased production of reactive oxygen species (ROS) [21–23] and methane dicarboxylic aldehyde (MDA) [24] are often accompanied with oxidative stress. Thus, a disruption of various signal transduction pathways is the main underlying mechanism of cell injury [25–29]. Among these signalling pathways, mitogen-activated protein kinase (MAPK)/extracellular signal-regulated kinase (ERK) signalling is a well-studied pathway involving the regulation of oxidative stress-induced cell apoptosis and cell damage [30, 31].

ERK is a member of the mitogen-activated protein kinases (MAPKs) signalling cascade families, which includes the ERK1 and ERK2 subunits, with respective to the molecular weights of 44 and 42 kD [32]. ERK1 and ERK2 share 90 % homology and use the same substrate in vitro. These enzymes can be activated through phosphorylation by different extracellular irritants, such as mitogen, growth factors and oxidative stress [33]. The ERK signalling pathway plays a key role in the regulation of multiple cell functions, including cell proliferation, survival, apoptosis and migration [34]. In addition, several lines of evidence have suggested that the ERK signalling pathway could be activated in response to cell damage by oxidative stress in airway epithelial cells [35–37]. Mechanistically, oxygen-free radicals induce mitochondrial damage, accompanied with a release of cytochrome C (Cyt-C) into the cytoplasm, in which Cyt-C activates caspases, such as caspase-9 and caspase-3, eventually promoting cell apoptosis [38–40]. However, the BCL-2 family members are mitochondrial membrane anti-apoptotic proteins involved in the transformation of the mitochondria transmembrane potential [41]. The main anti-apoptotic proteins of BCL-2 family, such as Bcl-2 and Bcl-xl, inhibit the release of Cyt-C and protect cells from apoptosis by inhibiting the activation of caspases acting as downstream signals of Cyt-C. Notably, the activation of pro-apoptotic proteins also damages the structure and function of mitochondria [42]. Cell apoptosis could be induced by decreasing the expression and inactivation of ERK1/2, and by causing alterations in the expression of apoptosis-related genes. For example, an increased expression and activation of ERK1/2 delays the onset of apoptosis and increases the expression of Bcl-xl [43]. In contrast, the inhibition of ERK1/2 activity and expression could down-regulate the expression of the anti-apoptotic homologues Bcl-2 and Bcl-xl, although there is no effect on the expression of the pro-apoptotic protein Bak [44].

These results suggest that pathogen-induced oxidative stress is key for the pathogenesis of mycoplasma infection. Thus, we hypothesized that MAPK/ERK signalling might be involved in the cell death induced by *M. ovipneumoniae* infection in sheep airway epithelial cells. Therefore, we tested this hypothesis and examined the pathogen-host interaction of *M. ovipneumoniae* cells and normal sheep bronchial airway epithelial cells using an air-liquid interface (ALI) culture model. The results showed that an *M. ovipneumoniae* infection could induce oxidative stress and mitochondrial dysfunction in part through the MAPK/ERK signalling pathway in sheep airway epithelial cells.

Results

The cell death and mitochondrial dysfunction of sheep airway epithelial cells induced by *M. ovipneumoniae* infection

Upon cell death and plasma membrane damage, lactate dehydrogenase (LDH) is rapidly released into the cell culture medium, therefore accessing the free LDH used to quantify cell death in response to *M. ovipneumoniae* infection [45]. Compared with the uninfected control, the dose-dependent cytotoxicity of sheep airway epithelial cells was observed in response to *M. ovipneumoniae*. Consistent with our previous findings [27], 71.26 % of cell death was determined in sheep ALI airway epithelial cells infected by *M. ovipneumoniae* at an MOI of 100 (Fig. 1a). Importantly, the increased dose-dependent cell death was inversely correlated with a decreased mitochondrial membrane potential in *M. ovipneumoniae*-infected sheep airway epithelial cells based on the results of the JC-1 assay, which assesses the integrity of the mitochondrial membrane (Fig. 1b). JC-1 is a fluorescent probe for testing mitochondrial membrane potential. Compared with uninfected control cells, the fluorescent intensity ratios (red/green) of JC-1 in airway epithelial cells were decreased 3.76, 8.85 and 12.55 %, with increased M. *ovipneumoniae* infection at an MOI of 1, 10 and 100, respectively (Fig. 1b). Mechanistically, a decline in the mitochondrial membrane potential has been suggested as a symbolic event during early periods of apoptosis [46].

Effect of *M. ovipneumoniae* infection on the production of MDA and SOD

We next investigated whether the observed mitochondrial dysfunction resulted from oxidative stress induced by *M. ovipneumoniae* infection. To this end, we examined the

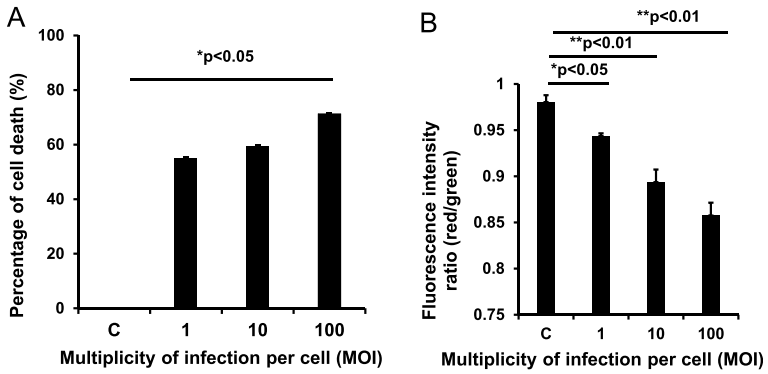

Fig. 1 Impact of M. *ovipneumoniae* infection on the cell death and mitochondrial membrane potential of sheep airway epithelial cells. Sheep airway epithelial cells cultured on an air-liquid interface model were apically infected with 1, 10 and 100 MOI of *M. ovipneumoniae* (MO) at 37 °C for 24 h. The cell viability was detected in terms of a LDH assay (**a**) and the mitochondrial membrane potential was determined using a potential-sensing fluorescent probe (JC-1) (**b**). **a** The percentage of cell death of ALI sheep airway epithelial cells infected with the indicated doses of MO, and a dose-dependent cell death was induced by MO infections. **b** Mitochondrial membrane potential (ΔΨm) of airway epithelial cells infected with indicated dose of MO, and the fluorescence intensity of both mitochondrial JC-1 monomers (λex 514 nm, λem 529 nm) and aggregates (λex 585 nm, λem 590 nm) were measured. The mitochondrial ΔΨm of airway epithelial cells were calculated as the fluorescence ratio of red over green. The mitochondrial ΔΨm decreased with increasing MOI of infection. Data were expressed as the means ± SD of three independent experiments, and each experiment had six replicated ALI cultures ($N = 18$). Compared with the uninfected controls, *: $p < 0.05$; **: $p < 0.01$. The cell numbers of each transwell with diameter of 24 mm was determined as 10^7

production of MDA and SOD, using MDA as an indicator of lipid peroxidation and a marker for oxidative stress. SOD is an important antioxidant enzyme that induces disproportionation by catalysing the superoxide anion, which could serve as an anti-oxidative marker. As expected, *M. ovipneumoniae* infection induced MDA generation and markedly increased MDA production by 30.2 % in cells infected with *M. ovipneumoniae* at an MOI of 100 compared with the uninfected control (Fig. 2a), suggesting that *M. ovipneumoniae* infection induced lipid peroxidation in sheep airway epithelial cells. In contrast, *M. ovipneumoniae* infection showed a dose-dependent decrease in SOD activity and expression (Fig. 2b). Compared with the control, *M. ovipneumoniae* infection at an MOI of 100 reduced the total SOD (T-SOD) activity by 22.6 % (Fig. 2b). In addition, the MDA/SOD ratio, an index of oxidative stress, was also dramatically increased with infection in a dose-dependent manner (Fig. 2c). Because Mn-SOD is a major antioxidant enzyme of T-SOD, distributed primarily throughout the mitochondrial matrix [47], the expression of Mn-SOD was also examined. Consistent with this notion, the Mn-SOD protein was significantly reduced in sheep airway epithelial cells following M. *ovipneumoniae* infection (Fig. 2d). These data suggest that *M. ovipneumoniae* can induce lipid peroxidation and oxidative stress in sheep airway epithelial cells.

The effect of *M. ovipneumoniae* infection on the production of CAT and GSS

Increased cellular ROS levels can damage proteins, lipids, and nucleic acids and reduce the activities of various antioxidant enzymes, such as CAT. Hence, we determined the activities of CAT in airway epithelial cells treated with *M. ovipneumoniae*. Compared with uninfected cells, a 10.4 % decrease in CAT activity was observed in airway epithelial cells infected with *M. ovipneumoniae* at an MOI of 100 (Fig. 3a). Moreover, glutathione synthetase (GSS), another antioxidant enzyme, was reduced in response to the increased ROS concentration. As expected, these results showed that the expression of GSS protein was significantly reduced in epithelial cells following an *M. ovipneumoniae* infection (Fig. 3b).

RAS/MEK/ERK is involved in sheep airway epithelial cells in response to *M. ovipneumoniae* infection

Accumulating evidence has shown that *M. ovipneumoniae* induces oxidative stress in airway epithelial cells. Previous studies have revealed that increased ROS production could induce oxidative stress [48] and impact the regulation of the RAS/MEK/ERK signalling pathway [49]. Thus, we next examined whether the ERK signalling was involved in *M. ovipneumoniae*-induced ROS generation. The airway epithelial cells were infected with *M. ovipneumoniae* at an MOI of 100 in the presence or absence of PD980025 (an ERK inhibitor). The ROS levels were detected using 2′,7′-dichlorofluorescein diacetate (DCFH-DA). The results showed that *M. ovipneumoniae* infection significantly increased ROS production in ALI cultures, while PD980025 markedly inhibited M. *ovipneumoniae*-induced ROS production (Fig. 4a), suggesting that the ERK signalling was involved in M. *ovipneumoniae*-induced ROS generation. In order to further understand the underlying mechanism of RAS/MEK/ERK signalling in airway epithelial cells in response to *M. ovipneumoniae*

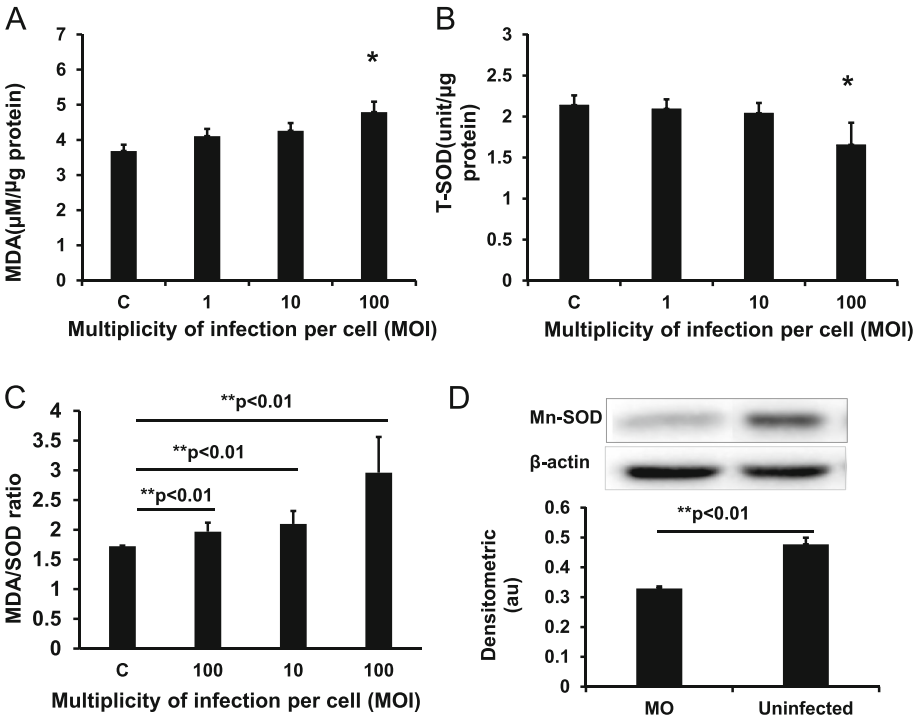

Fig. 2 Effects of *M. ovipneumoniae* infections on the production of MDA and SOD in sheep airway epithelial cells. Sheep airway epithelial cells cultured on an air-liquid interface model were apically infected with 1, 10 and 100 MOI of *M. ovipneumoniae* (MO) at 37 °C for 24 h, the levels of MDA and SOD were measured using appropriate kits. **a** A dose-dependent increase of MDA production was observed in cells infected with MO. **b** A dose-dependent decrease of total-SOD (T-SOD) level of airway epithelial cells was induced by the MO infection. **c** A significant increase in the MDA/SOD ratio in sheep airway epithelial cells infected with MO. **d** A representative image of immunoblot showing the reduced expression of Mn-SOD protein in ALI cultures infected with MO (MOI = 100) (*top panel*) compared with the uninfected cells, which was significantly different as determined based on the value of densitometric arbitrary units (A.U.) calculated as the densitometric signal of Mn-SOD protein over that of the corresponding β-actin internal control (*bottom panel*). Data were expressed as the means ± SD from three independent experiments, and each experimental had six replicated ALI cultures ($N = 18$) in **a**–**c**. Compared with the uninfected controls, *: $p < 0.05$; **: $p < 0.01$. The cell numbers of each transwell with diameter of 24 mm was determined as 10^7

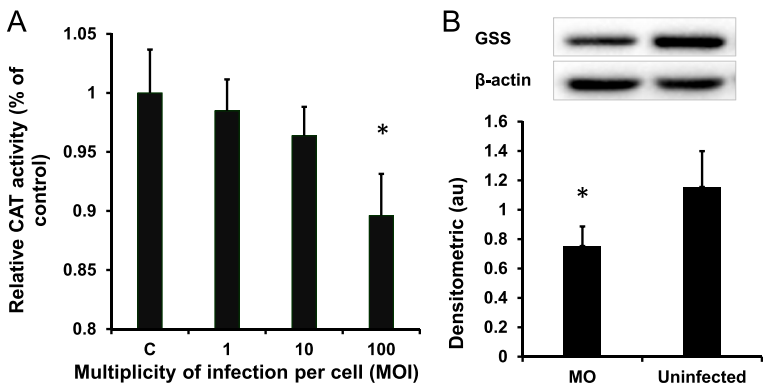

Fig. 3 Effects of *M. ovipneumoniae* infections on CAT activity and GSS expression. Sheep airway epithelial cells cultured on an air-liquid interface model were apically infected with 1, 10 and 100 MOI of *M. ovipneumoniae* (MO) at 37 °C for 24 h, and the activities of CAT and GSS expression were determined. **a** A dose-dependent decrease of CAT activity was observed in airway epithelial cells infected with MO. **b** A representative image of immunoblot showed the reduced expression of GSS protein in ALI cells infected with MO (MOI = 100) (*top panel*) compared with the uninfected cells, which was significantly different based on the value of densitometric arbitrary units (A.U.), which was calculated based on densitometric signal of GSS protein over that of the corresponding β-actin internal control (*bottom panel*). Data were expressed as the means ± SD from three independent experiments, with each experimental had six replicated ALI cultures ($N = 18$) in A. Compared with the uninfected controls, *: $p < 0.05$; **: $p < 0.01$. The cell numbers of each transwell with diameter of 24 mm was determined as 10^7

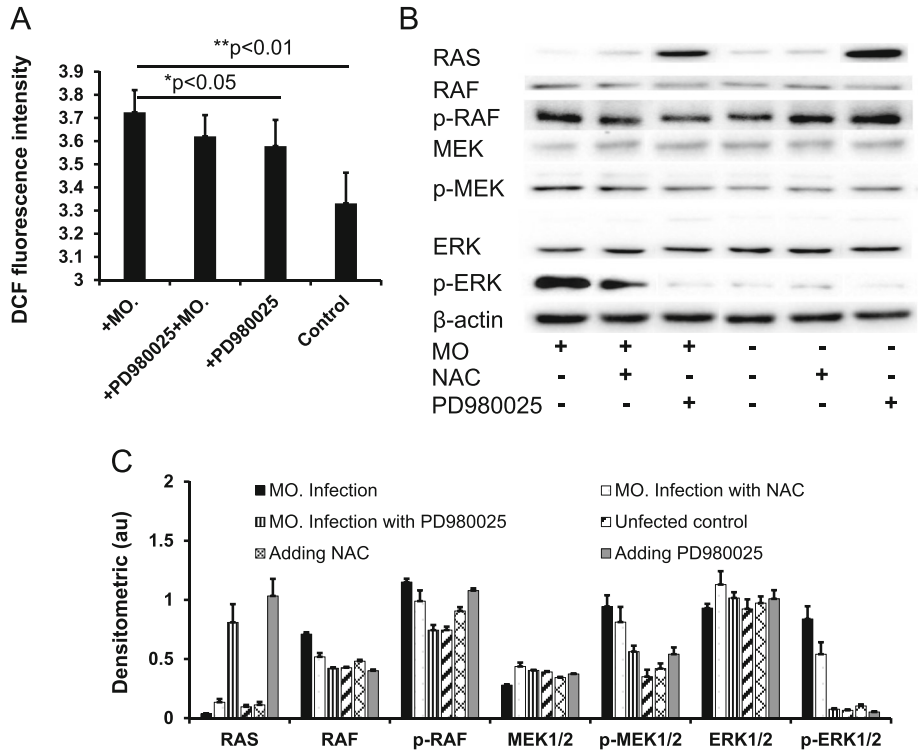

Fig. 4 The production of ROS and expression of MEK/ERK signalling in sheep airway epithelial cells induced by M. *ovipneumoniae* infection. Sheep airway epithelial cells cultured on an air-liquid interface model were apically infected with *M. ovipneumoniae* (MO) at an MOI of 100 for 24 h, and the production of ROS was measured by a fluorometrical assay using DCFH-DA dye (**a**), and changes in the expression of key molecules of the MEK/ERK signalling pathway was assessed using an immunoblotting method. **a** An infection of MO led an increased production of ROS in airway epithelial cells, which could be partially inhibited by MEK/ERK signalling inhibitor PD980025. **b** An immunoblotting assay revealed an evoked expression of RAS, RAF, p-RAF, MEK, p-MEK, ERK and p-ERK proteins in cells infected with MO, and this induction was inhibited PD980025 and ROS scavenger NAC. **c** Semi-quantitative analysis of the expression of proteins in (**b**) by evaluating the relative densitometric densities using arbitrary units (A.U.), calculated according to the densitometric signal of a protein of interest over that of the corresponding β-actin internal control. Data were expressed as the mean ± SD from three independent experiments. Compared to the uninfected controls, *: $p < 0.05$; **: $p < 0.01$ in cells untreated with PD980025. The cell numbers of each transwell with diameter of 24 mm was determined as 10^7

infection, an immunoblotting assay was employed to analyse the RAS, RAF, phosphorylated-RAF (p-RAF), MEK, p-MEK, ERK and p-ERK proteins in airway epithelial cells in the presence or absence of NAC (a ROS scavenger) or PD980025 (Fig. 4b and c). The results showed that *M. ovipneumoniae* could activate the phosphorylation of RAS, MEK and ERK, while the presence of NAC or PD980025 remarkably inhibited the activation of phosphorylated RAS, MEK and ERK. These data clearly suggest that the activation of the RAS/MEK/ERK signalling pathway plays a major role in sheep airway epithelial cells in response to *M. ovipneumoniae* infection, which also impacts the increased ROS production in sheep airway epithelial cells following M. *ovipneumoniae* infection.

Sheep airway epithelial cell apoptosis induced by *M. ovipneumoniae* infection

In order to further reveal the potential molecular mechanism underlying the mitochondria damage of sheep airway epithelial cells induced by *M. ovipneumoniae* infection, the changes in BCL-2 family proteins and downstream Cyt-C and caspase signalling cascades were evaluated by an immunoblotting assay [41, 42]. The immunoblots showed that *M. ovipneumoniae* infections significantly inhibited the expression of Bcl-2, Bcl-xl and Bak but that it did not alter the expression of Bad (Fig. 5a and b). Interestingly, the addition of the ROS scavenger NAC significantly increased Bcl-2 and Bcl-xl protein levels, regardless of M. *ovipneumoniae* infection, suggesting that the *M. ovipneumoniae*-inhibited the expression of BCL-2 family members in part by producing ROS in airway epithelial cells (Fig. 5a and b). In addition, BCL-2 family members are downstream genes of the ERK signalling pathway; thus, we examined the effect of *M. ovipneumoniae*-activated phosphorylated ERK on the expression of BCL-2 family proteins. Interestingly, the presence of the ERK inhibitor PD980025 restored the expression of BCL-2 family members following *M. ovipneumoniae* infection in sheep airway epithelial cells (Fig. 5a and b), indicating that *M. ovipneumoniae* induces mitochondrial dysfunction by

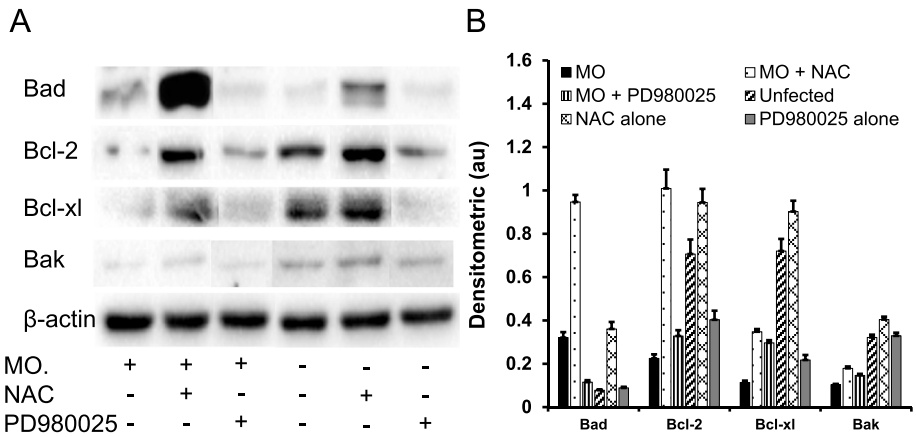

Fig. 5 Induction of the expression of BCL-2 family in sheep airway epithelial cells infected with M. *ovipneumoniae*. Sheep airway epithelial cells cultured on an air-liquid interface model were apically infected with *M. ovipneumoniae* (MO) at an MOI of 100 for 24 h, changes in the expression of BCL-2 family members was assessed using an immunoblotting assay. **a** Representative images of immunoblots of indicated proteins, revealed an evoked expression of pro-apoptotic proteins Bad, Bcl-2, Bcl-xl and Bak, and the MO-induced expression of these proteins could be diminished by MEK/ERK signalling PD980025 or ROS scavenger NAC. **b** Semi-quantitative analysis of the expression of proteins in (**a**) by evaluating relative densitometric densities using arbitrary units (A.U.), calculated based on the densitometric signal of a protein of interest over that of the corresponding β-actin internal control

inhibiting the anti-apoptosis proteins, Bcl-2 and Bcl-xl, through mechanisms involving ROS production and the ERK signalling pathway.

The release of Cyt-C is another hallmark of mitochondrial dysfunction and cell apoptosis [39], immunoblotting analysis also showed a strikingly increased abundance of Cyt-C in airway epithelial cells following *M. ovipneumoniae* infection, and the addition of NAC or PD980025 significantly decreased Cyt-C release (Fig. 6a and b). Consequently, increased cytosol Cyt-C triggers the activation of the caspase cascade and cell apoptosis [40]. Immunoblot analysis showed that *M. ovipneumoniae* infection significantly increased the expression of p35-caspase-9 and p17-caspase-3 and decreased the expression of p32-caspase-3 (Fig. 7a and b). In contrast, the expression of p35-caspase-9 increased, but the expression of p17-caspase-3 and p32-caspase-3 decreased in the presence of ROS scavenger NAC (Fig. 7a and b). Similarly, the decreased expression of p35-caspase-9 and p32-caspase-3 was observed in cells exposed to the ERK inhibitor PD980025 (Fig. 7a and b). These data suggest that *M. ovipneumoniae* infection could induce the release of Cyt-C into the cytoplasm and activate caspase-9 and caspase-3 signalling cascades through mechanisms involving ROS production and ERK signalling pathways.

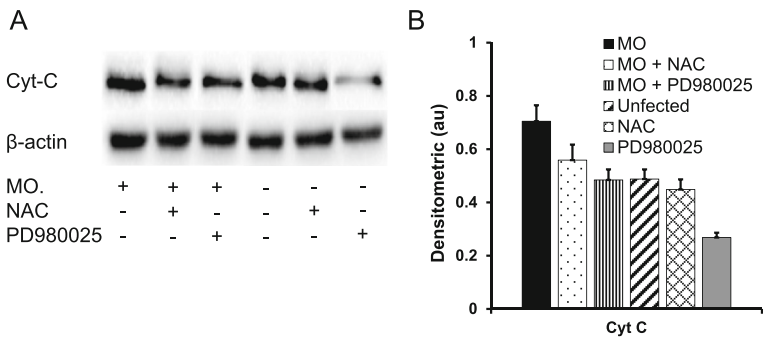

Fig. 6 Induction of the expression of Cyt-c in sheep airway epithelial cells infected with M. *ovipneumoniae*. Sheep airway epithelial cells cultured on an air-liquid interface model were apically infected with *M. ovipneumoniae* (MO) at an MOI of 100 for 24 h, changes in the expression of mitochondrial Cyt-c were assessed by an immunoblotting assay. **a** Representative images of immunoblots of Cyt-c and β-actin, revealed an increased release of Cyt-c in cells infected with MO, and the increased level of Cyt-c was reduced in the presence of MEK/ERK signalling PD980025 or ROS scavenger NAC. **b** Semi-quantitative analysis of the expression of proteins in (**a**) by evaluating relative densitometric densities using arbitrary units (A.U.), which was calculated with densitometric signal of a protein of interest over that of the corresponding β-actin internal control

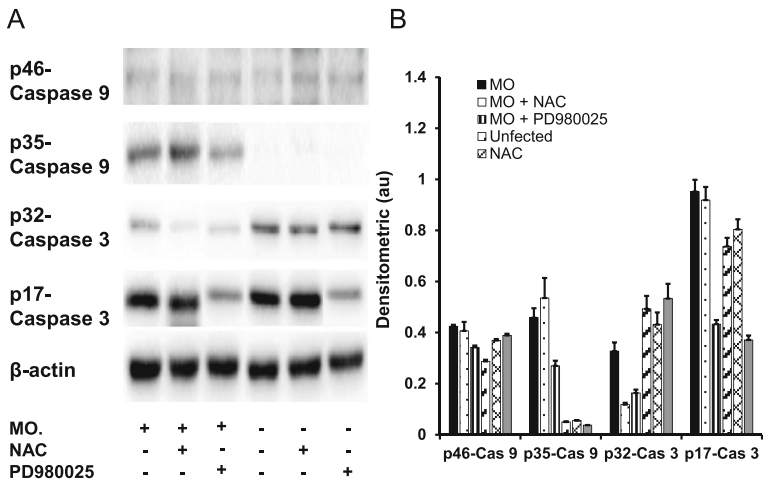

Fig. 7 Induction of the expression of caspase-3/9 in sheep airway epithelial cells infected with M. *ovipneumoniae*. Sheep airway epithelial cells cultured on an air-liquid interface model were apically infected with *M. ovipneumoniae* (MO) at an MOI of 100 for 24 h, changes of the expression of caspases was assessed using an immunoblotting assay. **a** Representative images of immunoblots of indicated caspases or their activated forms, revealed an enhanced activities of caspase 3 and 9 in airway epithelial cells infected with MO, and an addition of MEK/ERK signalling PD980025 or ROS scavenger NAC resulted in reducing the MO-induced activities of these caspases. **b** Semi-quantitative analysis of the expression of proteins in (**a**) by evaluating the relative densitometric densities using arbitrary units (A.U.), calculated based on the densitometric signal of a protein of interest over that of the corresponding β-actin internal control

Discussion

We previously described MyD88-dependent toll-like receptor (TLR) signalling induced by *M. ovipneumoniae* in sheep airway epithelial cells [27]. In the present study, we examined the underlying mechanism of airway epithelial cell death induced by *M. ovipneumoniae* infection using an ALI culture model. The results showed that *M. ovipneumoniae* infection induces ROS production, cell death and mitochondrial membrane dysfunction and increased MDA concentration but decreased the expression of antioxidant enzymes CAT, GSS, T-SOD and Mn-SOD. Mechanistically, the *M. ovipneumoniae*-induced cell death and mitochondrial dysfunction in part reflected mechanisms by which the pathogen activates RAS/MEK/ERK signalling, leading to mitochondrial damage and Cyt-C release into the cytoplasm, which in turn triggers the activation of the caspase signalling cascade, eventually leading to host cell apoptosis.

In the present study, an ALI culture model generated using primary sheep bronchial epithelial cells was employed to assess the pathogen-host interaction between *M. ovipneumoniae* and airway epithelial cells. The epithelial cells cultured in an ALI status fully differentiated into distinct epithelial cell types and formed a pseudostratified epithelium comprising tight junctions. The apical cell surface represented an environment comparable to the airway lumen in vivo [27, 50]. By using this novel model, the mechanism of *M. ovipneumoniae*-induced oxidative stress in sheep airway epithelial cell was explored. In the present context, *M. ovipneumoniae* induced the generation of ROS and reduced the expression and activity of antioxidant enzymes, including T-SOD, Mn-SOD, CAT and GSS, suggesting that oxidative stress was induced by *M. ovipneumoniae* in sheep airway epithelial cells. For example, Mn-SOD is one of the primary defence substances in mitochondria and is located in the mitochondrial matrix. Notably, reduced Mn-SOD activity is correlated with the lack of mitochondrial defence [47]. Therefore, a decreased mitochondrial membrane potential in airway epithelial cells following the *M. ovipneumoniae* infection suggests that the pathogen induces oxidative stress to injure mitochondria, which sequentially triggers a mechanism of mitochondrial damage. Similarly, the MDA is a marker of lipid peroxide, which reduces member fluidity and induces cell apoptosis [51]. Consistent with this notion, the increased concentration of MDA and ROS was observed in cells infected with *M. ovipneumoniae*, accompanied with the reduced expression and inactivation of antioxidant enzymes, as well as the dysfunction and disruption of the mitochondrial membrane structure in host cells, evidenced by a decreased mitochondrial membrane potential.

The BCL-2 family members are closely related to mitochondrial membrane integrity, of which Bcl-2 and Bcl-xl are anti-apoptotic factors of this family. In the present study, the expression of Bcl-2, Bcl-xl and Bak in sheep airway epithelial cells was inhibited in cells infected by *M. ovipneumoniae*, indicating that an apoptotic event might occur in these infected cells [42, 52]. Bak is an interesting member of the BCL-2 family, which can exert both pro-apoptotic and anti-apoptotic roles in a cell context-dependent manner [53]. The reduced expression of Bak in

M. ovipneumoniae-infected cells might suggest that this enzyme plays an anti-apoptotic role in the *M. ovipneumoniae*-induced mitochondrial damage mechanism. In order to investigate whether *M. ovipneumoniae*-induced oxidative stress impacts the expression of BCL-2 family proteins, cells infected with *M. ovipneumoniae* were treated with the ROS scavenger NAC. Interestingly, *M. ovipneumoniae*-reduced the expression of Bcl-2 and Bcl-xl proteins in airway epithelial cells, and this expression was restored after the addition of NAC. Notably, *M. ovipneumoniae* infection did not significantly alter the expression of Bad, likely reflecting the location of Bad in epithelial cells, as this protein was not consistently located on mitochondria in a cell type-dependent context and could be activated and translocated to mitochondria [42].

The transformation of the mitochondrial membrane potential can convert the transformation of the membrane permeability [46] through a mechanism involving the release of cytochrome C (Cyt-C) [38] and the activation of the caspase 3/9 cascade [39, 40]. In the present study, the increased release of Cyt-C and activation of caspase3/9 signalling were observed in *M. ovipneumoniae*-infected sheep airway epithelial cells, suggesting that a mitochondria-related signalling pathway was involved in the *M. ovipneumoniae*-induced apoptosis of epithelial cells. Equally noteworthy, the release of Cyt-C and activation of caspase 3/9 reflected *M. ovipneumoniae*-induced oxidative stress, consistent with evidence that the ROS scavenger NAC could suppress Cyt-C release and caspase-3 activation in *M. ovipneumoniae*-infected airway epithelial cells. However, NAC had no effect on caspase-9 activation, consistent with a previous study showing that the activation of caspase-9 was not dependent on the concentration of cytoplasmic Cyt-C [54]. Therefore, these findings suggested that the *M. ovipneumoniae*-induced mitochondrial damage most likely depended on the levels of cytoplasm cytochrome C in airway epithelial cells.

In addition, mitochondrial signalling occurs downstream of the ERK signalling pathway. Therefore, targeting ERK signalling might impact the mitochondria-related apoptotic signalling pathway. Indeed, the inhibition of ERK signalling using PD980025 restored the expression of anti-apoptotic BCL-2 family proteins, and suppressed Cyt-C release and caspase 3/9 activation in *M. ovipneumoniae*-infected sheep airway epithelial cells. Together with evidence that ROS activates ERK signalling and *M. ovipneumoniae* infection activates the RAS/MEK/ERK signalling pathway, these data suggested that the mitochondria signalling pathway was mediated by the RAS/MEK/ERK signalling in sheep airway epithelial cells in response to *M. ovipneumoniae* infections.

Interestingly, glycerol metabolism has been implicated in the generation of H2O2 and ROS in many mycoplasma species [9–11, 55]. However, there are no data concerning the involvement of glycerol metabolism in the production of ROS and H_2O_2 for *M. ovipneumoniae*, although the genome sequence of the *M. ovipneumoniae* SC1 strain was completed in 2011 [56]. Thus, the role of glycerol metabolism in *M. ovipneumoniae*-induced oxidative stress warrants further investigation in the future.

Conclusions

In the present study, we attempted to uncover the mechanism underlying the pathogen-host interaction between *M. ovipneumoniae* and sheep airway epithelial cells using an ALI culture model. The results demonstrated a mechanism of cell death-regulated signalling pathways in mitochondria of airway epithelial cells in response to Mycoplasma infections (Fig. 8) [57], by which a *M. ovipneumoniae* infection could induce oxidative stress by increasing production of ROS and lipid peroxidation, and the inhibition of antioxidant enzyme activity in airway epithelial cells. Mechanistically, *M. ovipneumoniae* bacteria activate RAS/MEK/ERK signalling, which disrupted the integrity of mitochondrial membrane through the reduction of the expression of BCL-2 family anti-apoptotic proteins, increasing the release of Cyt-C and activating the caspase signalling cascade, thus sequentially inducing cell apoptosis.

Methods

Propagation of *Mycoplasma Ovipneumoniae*

The *M. ovipneumoniae* Queensland Strain Y98 [58] was obtained from the China Institute of Veterinary Drug Control (Beijing, China). As previously described [58], the mycoplasma bacterium was cultured and propagated in a mycoplasma broth containing mycoplasma broth base CM403, supplement-G SR59 (OXOID, Hampshire, UK), 0.5 % glucose, and 0.002 % phenol red at 37 °C in 1 % CO_2. The titre of *M. ovipneumoniae* culture was determined based on the metabolic activity of the bacterial cells in the medium, presented as a colour change unit (CCU)/mL [59]. The CCU assay is accurate and comparable to traditional colony formation units (CFU) on agar plates for the titration of mycoplasma species, although the results of this assay might provide a higher estimate of cell numbers, consistent with the DNA content of the cell pellet and published genome sizes [60, 61]. Prior to use, the bacterial cells were washed three times in PBS in order to minimize the effects of potential contaminants originating from the culture medium (e.g., LPS or other molecules).

In vitro ALI culture of sheep bronchial epithelium and infection

The present study was approved by the ethics committee for the use of animals at Ningxia University. The bronchi

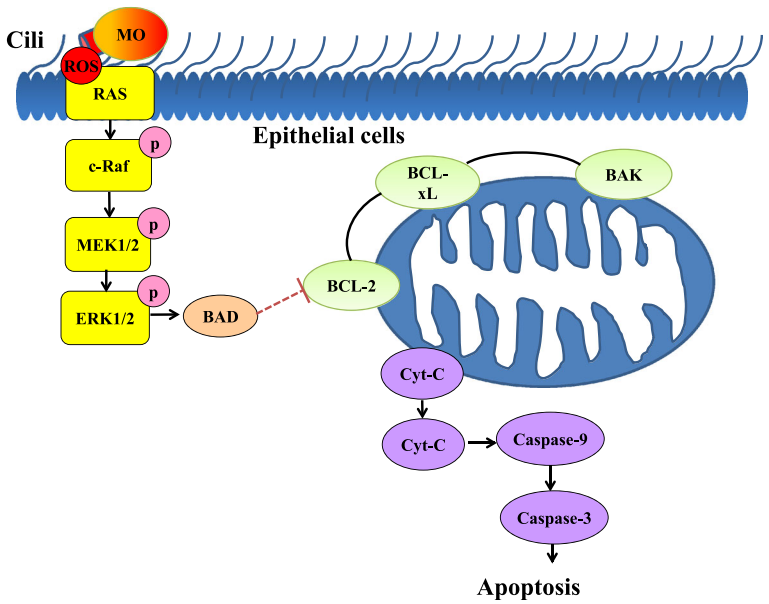

Fig. 8 Schematic diagram of an apoptotic cell death induced by M. *ovipneumoniae* infection via signalling pathways converging at mitochondria. An infection of *M. ovipneumoniae* generated ROS triggers the activation of ERK signalling of sheep airway epithelial cells, which induce cell apoptosis through an ERK signalling-mediated mitochondria pathway

of Chinese Tan sheep (*O. aries*) (1.5 to 2.0 years old) were obtained from a local slaughterhouse. Despite the need for consent is deemed unnecessary according to national regulations, an informed verbal consent was obtained from the sheep owners. The ethics committee for the use of animals of Ningxia University approved this study. The ALI culture of airway epithelial cells was generated as previously described [27]. Briefly, the bronchus was longitudinally opened after the muscle and vascular tissues were removed and washed in ice-cold 1 % Pen Strep–1.0 g/mL fungizone PBS. Then, the bronchial specimens were incubated in a tube filled with epithelial cell dissociation buffer (DMEM Pen Strep–fungizone medium containing 1.5 mg/mL pronase and 10 μg/mL DNase I) at 4 °C for 24–36 h, with rotation during dissociation. The enzymatic dissociation was terminated by adding FBS at a final concentration of 10 %, and the epithelial cells were then collected by centrifugation at 500 *g* for 10 min at 4 °C as previously described [4]. The cell pellet was re-suspended in DMEM 5 % FBS, followed by incubating the cells on tissue culture plates (Primera; Becton-Dickinson Labware, Franklin Lakes, NJ) for 2–4 h in 5.5 % CO_2 at 37 °C for the adhesion of fibroblasts, after which the non-adherent cells were collected by centrifugation and re-suspended in Bronchial Epithelial cell Growth Medium (BEGM) (Lonza, Basel, Switzerland). The number of total cells was determined using a haemocytometer counting chamber. In vitro, ALI cultures of sheep bronchial epithelial cells were cultured previously described [50]. Briefly, the polycarbonate/polyester porous (0.4 μM pores) transwell membranes (PCF Millicell inserts, Millipore, Bedford, MA) were pre-coated with 60 μg/mL of type I rat tail collagen (BD Biosciences, San Jose, CA, USA). Approximately 1×10^5 cells were seeded into a 0.6 cm^2 Millicell insert membrane, and subsequently the inserts were incubated in BEGM medium (containing 5 % FBS) in the apical and basolateral compartment of a 24-well plate at 37 °C in 6 % CO_2 for approximately 18–24 h. Then, the membranes were washed with pre-warmed PBS to remove unattached cells and re-fed with BEGM medium and cultured for 2 additional days. To establish an air–liquid interface, 2 % Ultroser G (USG) medium (Pall, Port Washington, NY, USA) was added to the basolateral side of the chamber. The medium was refreshed twice a week, and the top of the membrane culture remained visibly dry. The polarized and highly differentiated airway epithelial cell layer was achieved after 2 weeks of ALI culture. For a 2.4-cm diameter Millicell insert membrane, 1×10^7 well-differentiated epithelial cells were determined [50]. A well-differentiated 4-week ALI culture was used for infection. For infection, *M. ovipneumoniae* cells were suspended, diluted in 2 % Ultroser G medium, and applied on the apical surface of ALI epithelial cells for infection at the indicated time periods, and an equal volume of 2 % Ultroser G medium was used as an uninfected control. Volumes of 0.5 and 0.1 mL were employed to cover the wells at diameters of 2.4 and 1.2 cm, respectively.

LDH assay

Cell death was measured using a lactate dehydrogenase (LDH) assay based on the detection of the LDH released from injured cells. Mechanistically, LDH can oxidize lactate to generate NADH, which in turn reacts with INT, determined as a yellow coloured substrate with maximum absorbance at 450 nm (Beyotime Company, Jiangsu, China). The 6-week ALI cultures were infected at a multiplicity of infection (MOI) of 1, 10 and 100 per *M. ovipneumoniae* cell through the application of bacterial cells on the apical surface of cultures for 24 h and then incubated with LDH staining solution at 37 °C for 1 h. Then, the supernatant was used to examine the relative LDH activity using a Tecan Safire 5 microplate reader (450 nm).

Mitochondrial membrane potential (MMP) assay

The integrity of the mitochondrial membrane was evaluated based on the mitochondrial membrane potential (MMP) using a JC-1 fluorescent probe. In normal cells, JC-1 exists as a monomer (green) in the cytosol and accumulates as aggregates (red) in mitochondria through the induction of higher MMP. In apoptotic and necrotic cells, JC-1 remains in the monomeric form and stains as green fluorescence in the cytosol. The 6-weeks ALI cultures were infected with MOI of 1, 10 and 100 of *M. ovipneumoniae* by applying the bacterial cells on the apical surface for 24 h and then incubated with JC-1 (Beyotime Company, Jiangsu, China) staining solution (5 μg/mL) at 37 °C for 20 min. The fluorescence intensity of both mitochondrial JC-1 monomers (λ_{ex} 514 nm and λ_{em} 529 nm) and aggregates (λ_{ex} 585 nm and λ_{em} 590 nm) was detected using a Tecan Safire 5 microplate reader. The $\Delta\Psi_m$ of the cells was calculated as the fluorescence ratio of red to green.

Measurement of MDA and SOD

The MDA concentration was determined using a thiobarbituric acid (TBA) test as previously described [62]. MDA reacts with TBA to form MDA-(TBA), a red adduct with a maximum absorbance at 532 nm (Beyotime Company, Jiangsu, China). For the MDA measurement, the cell lysates were added to the MDA detection solution and boiled for 15 min, followed by centrifugation at 1000 *g* for 10 min. Then, the supernatant was used to examine the relative MDA units using a Tecan Safire 5 microplate reader at a wavelength of 532 nm. Total SOD (T-SOD) activity was detected using SOD assay kits according to the manufacturer's instructions (Beyotime Company, Jiangsu, China). Briefly, the cell lysates were mixed with nitroblue tetrazolium (NBT) and enzyme working solutions and incubated at 37 °C for 20 min. The absorbance of T-SOD was recorded at 560 nm using a Tecan Safire 5 microplate reader.

Measurement of CAT

CAT activity was analysed according to the manufacturer's instructions (Beyotime Company, Jiangsu, China). The samples were treated with excessive hydrogen peroxide and incubated for 5 min. Then the hydrogen peroxide not decomposed by CAT was coupled with a substrate to produce N-4-antipyryl-3-chloro-5-sulfonate-p-benzoquinone-monoimine after peroxidase treatment, which has an absorption maximum of 520 nm. The CAT unit was defined as the amount of enzyme that catalysed 1 μM of H_2O_2 to H_2O and O_2 per min at 25 °C.

ROS assay

The concentration of ROS was fluorometrically monitored using DCFH-DA. The cells were treated with MEK inhibitor PD980025 (Sigma, USA) for 24 h prior to *M. ovipneumoniae* infection at an MOI of 100 through the application of the bacterial cells on the apical surface, followed by incubation at 37 °C overnight in 24-well plates. After the membranes were washed three times with PBS, DCFH-DA was diluted in fresh phenol red-free DMEM to a final concentration of 5 μM and incubated with the cells at 37 °C for 20 min. The chemicals were then removed, and the cells were washed three times. Relative ROS units were determined using a Tecan Safire 5 microplate reader (λex 485 nm and λem 530 nm). Changes in the ROS concentration were expressed as a percentage over the control.

Immunoblotting analysis

Whole cell extracts were prepared by homogenizing cells in lysis buffer (50 mM Tris–HCl, pH 7.5, 5 mM EDTA, 150 mM NaCl, and 0.5 % NP-40) for 60 min on ice. The soluble protein concentration was measured with Bio-Rad Protein Assay (Bio-Rad Laboratories, Richmond, CA, USA). The resulting clarified lysates (100 μg) were separated using 8 % or 10 % sodium dodecyl sulphate (SDS)-polyacrylamide gel (SDS-PAGE) and transferred to nitrocellulose membranes for immunoblotting assay against antigen-specific antibodies. The membrane was blocked with 5 % fat-free dry milk in PBS containing 0.2 % Tween-20, and probed with antibodies against the protein of interest. The antibodies used in the present study included rabbit anti-SOD2, rabbit anti-RRAS, rabbit anti-RAF1, rabbit anti-ERK1/2, rabbit anti-BAK, rabbit anti-BAD, rabbit anti-BCL2, rabbit anti-Caspase 3, rabbit anti-Caspase 9, rabbit anti-Cytochrome c (Cyt-C) (Proteintech Group, Campbell Park, Chicago, USA), rabbit anti-phosphorylated Raf1 (p-Raf1), rabbit anti-MEK1/2, rabbit anti-phosphorylated MEK1/MEK2 (p-MEK1/2), rabbit anti-phosphorylated ERK1/2 (p-ERK1/2) (Signalway Antibody, MD, USA), rabbit anti-GSS (ABGENT, San Diego, USA) and mouse anti-β-actin. These primary antibodies were applied at a dilution of 1:1000. Following

extensive washing, the membranes were incubated with an appropriate HRP-labelled secondary antibody. The blots were then developed using the enhanced Western Bright ECL reagent (Advansta, Menlo Park, CA, United States). The levels of protein expression were semi-quantified by optical densitometry using ImageJ Software version 1.46 (http://rsb.info.nih.gov/ij/). The ratio between the net intensity of each sample divided by the β-actin internal control was calculated as a densitometric arbitrary unit (A.U.), which served as an index of the relative expression of the protein of interest.

Statistical analysis

The data were obtained from at least three independent experiments for each experimental condition and presented as the means ± standard deviation (SD). The statistical significance was analysed using one-way ANOVA, followed by Tukey's multiple comparison test.

Additional file

Additional file 1: Original images of immunoblots for Figure 4B and Figure 5A. (PDF 860 kb)

Abbreviations

A.U.: Arbitrary unit; ALI: Air-liquid interface; BEGM: Bronchial epithelial cell Growth Medium; CAT: Catalase; CCU: Colour change unit; Cyt-C: Cytochrome C; DCFH-DA: 2′,7′-dichlorofluorescein diacetate; ERK: Extracellular signal-regulated kinase; GSS: Glutathione synthetase; LDH: Lactate dehydrogenase; MAPKs: Mitogen-activated protein kinases; MDA: Methane dicarboxylic aldehyde; MMP: Mitochondrial membrane potential; MO: *M. ovipneumoniae*/*Mycoplasma ovipneumoniae*; MOI: Multiplicity of infection; NAC: N-acetyl-L-cysteine; NBT: Nitroblue tetrazolium; p-ERK1/2: phosphorylated ERK1/2; p-MEK1/2: phosphorylated MEK1/MEK2; p-Raf1: Phosphorylated Raf1; ROS: Reactive oxygen species; SD: Standard deviation; SDS: Sodium dodecyl sulfate; SDS-PAGE: (SDS)-polyacrylamide gel; SOD: Superoxide dismutase; TBA: Thiobarbituric acid; TLR: Toll-like receptor; T-SOD: Total SOD; USG: Ultroser G

Acknowledgements

The authors thank Mr. Fuyang Song for technical assistance with the cytometric analysis, and Ms. Hui Yang and Ms. Jin Zeng for valuable discussions and assistance.

Funding

This work was financially supported by the National Key Basic Research Program of China (973 Program) (nos. 2012BAD12B07 and 2012CB518801) and the National Natural Science Foundation of China (nos. 31572494 and 31460660). The funders had no role in study design, data collection and analysis, decision to publish, or preparation of the manuscript.

Availability of data and materials

All the data supporting our findings are contained within the article and its Additional file 1.

Authors' contributions

YL, XL and YW conceived and designed the experiments; YL, ZJ, DX and GD analysed the data and drafted the manuscript; YL, ZJ and ML performed the experiments and acquired the data; and YW and XL interpreted the data and critically revised the manuscript. All authors read and approved the final version of the manuscript.

Competing interests

The authors declare that they have no competing interests.

Consent for publication

Not applicable.

Ethics approval and consent to participate

The experiments involving sheep were performed according to protocols approved by the Institutional Animal Care and Use Committee of Ningxia University (NXU-2014-007). The need for consent is deemed unnecessary according to national regulations, but an informed verbal consent was obtained from the sheep owners. The ethics committee for the use of animals of Ningxia University approved this study.

Author details

[1]Key Laboratory of Ministry of Education for Conservation and Utilization of Special Biological Resources in the Western, Yinchuan, Ningxia 750021, China. [2]College of Life Science, Ningxia University, Yinchuan, Ningxia 750021, China. [3]Ningxia Key Laboratory of Clinical and Pathogenic Microbiology, the General Hospital of Ningxia Medical University, Yinchuan, Ningxia 750004, China.

Received: 12 February 2016 Accepted: 17 September 2016
Published online: 23 September 2016

References

1. Mackay J, Nisbet D, Foggie A. Isolation of pleuropneumonia-like organisms (Genus Mycoplasma) from case of sheep pulmonary adenomatosis (SP A). Vet Rec. 1963;75(21):550–1.
2. Eckerle I, Ehlen L, Kallies R, Wollny R, Corman VM, Cottontail VM, Tschapka M, Oppong S, Drosten C, Muller MA. Bat airway epithelial cells: a novel tool for the study of zoonotic viruses. PLoS One. 2014;9(1):e84679.
3. Olson N, Hristova M, Heintz NH, Lounsbury KM, van der Vliet A. Activation of hypoxia-inducible factor-1 protects airway epithelium against oxidant-induced barrier dysfunction. Am J Physiol Lung Cell Mol Physiol. 2011;301(6):L993–L1002.
4. Liu X, Luo M, Zhang L, Ding W, Yan Z, Engelhardt JF. Bioelectric properties of chloride channels in human, pig, ferret, and mouse airway epithelia. Am J Respir Cell Mol Biol. 2007;36(3):313–23.
5. Jones GE, Keir WA, Gilmour JS. The pathogenicity of *Mycoplasma ovipneumoniae* and *Mycoplasma arginini* in ovine and caprine tracheal organ cultures. J Comp Pathol. 1985;95(4):477–87.
6. Abdul-Wahab OM, Ross G, Bradbury JM. Pathogenicity and cytadherence of *Mycoplasma imitans* in chicken and duck embryo tracheal organ cultures. Infect Immun. 1996;64(2):563–8.
7. Hatchel JM, Balish MF. Attachment organelle ultrastructure correlates with phylogeny, not gliding motility properties, in *Mycoplasma pneumoniae* relatives. Microbiology. 2008;154(Pt 1):286–95.
8. Bischof DF, Janis C, Vilei EM, Bertoni G, Frey J. Cytotoxicity of *Mycoplasma mycoides* subsp. mycoides small colony type to bovine epithelial cells. Infect Immun. 2008;76(1):263–9.
9. Maenpuen S, Watthaisong P, Supon P, Sucharitakul J, Parsonage D, Karplus PA, Claiborne A, Chaiyen P. Kinetic mechanism of L-alpha-glycerophosphate oxidase from *Mycoplasma pneumoniae*. FEBS J. 2015;282(16):3043–59.
10. Pritchard RE, Balish MF. *Mycoplasma iowae*: relationships among oxygen, virulence, and protection from oxidative stress. Vet Res. 2015;46:36.
11. Pritchard RE, Prassinos AJ, Osborne JD, Raviv Z, Balish MF. Reduction of hydrogen peroxide accumulation and toxicity by a catalase from *Mycoplasma iowae*. PLoS One. 2014;9(8):e105188.
12. Szczepanek SM, Boccaccio M, Pflaum K, Liao X, Geary SJ. Hydrogen peroxide production from glycerol metabolism is dispensable for virulence of *Mycoplasma gallisepticum* in the tracheas of chickens. Infect Immun. 2014;82(12):4915–20.
13. Valko M, Leibfritz D, Moncol J, Cronin MT, Mazur M, Telser J. Free radicals and antioxidants in normal physiological functions and human disease. Int J Biochem Cell Biol. 2007;39(1):44–84.
14. Ahmad S, White CW, Chang LY, Schneider BK, Allen CB. Glutamine protects mitochondrial structure and function in oxygen toxicity. Am J Physiol Lung Cell Mol Physiol. 2001;280(4):L779–791.
15. Berman SB, Hastings TG. Dopamine oxidation alters mitochondrial respiration and induces permeability transition in brain mitochondria: implications for Parkinson's disease. J Neurochem. 1999;73(3):1127–37.
16. Chen JR, Weng CN, Ho TY, Cheng IC, Lai SS. Identification of the copper-zinc superoxide dismutase activity in *Mycoplasma hyopneumoniae*. Vet Microbiol. 2000;73(4):301–10.

17. Willekens H, Chamnongpol S, Davey M, Schraudner M, Langebartels C, Van Montagu M, Inze D, Van Camp W. Catalase is a sink for H2O2 and is indispensable for stress defence in C3 plants. EMBO J. 1997;16(16):4806–16.
18. Simmons WL, Dybvig K. Catalase Enhances Growth and Biofilm Production of *Mycoplasma pneumoniae*. Curr Microbiol. 2015;71(2):190–4.
19. Avsian-Kretchmer O, Eshdat Y, Gueta-Dahan Y, Ben-Hayyim G. Regulation of stress-induced phospholipid hydroperoxide glutathione peroxidase expression in citrus. Planta. 1999;209(4):469–77.
20. Vitula F, Peckova L, Bandouchova H, Pohanka M, Novotny L, Jira D, Kral J, Ondracek K, Osickova J, Zendulkova D, et al. *Mycoplasma gallisepticum* infection in the grey partridge Perdix perdix: outbreak description, histopathology, biochemistry and antioxidant parameters. BMC Vet Res. 2011;7:34.
21. McCord JM, Fridovich I. Superoxide dismutase. An enzymic function for erythrocuprein (hemocuprein). J Biol Chem. 1969;244(22):6049–55.
22. Bai F, Ni B, Liu M, Feng Z, Xiong Q, Shao G. *Mycoplasma hyopneumoniae*-derived lipid-associated membrane proteins induce inflammation and apoptosis in porcine peripheral blood mononuclear cells in vitro. Vet Microbiol. 2015;175(1):58–67.
23. Ni B, Bai FF, Wei Y, Liu MJ, Feng ZX, Xiong QY, Hua LZ, Shao GQ. Apoptosis induced by lipid-associated membrane proteins from *Mycoplasma hyopneumoniae* in a porcine lung epithelial cell line with the involvement of caspase 3 and the MAPK pathway. Genet Mol Res. 2015;14(3):11429–43.
24. Romieu I, Barraza-Villarreal A, Escamilla-Nunez C, Almstrand AC, Diaz-Sanchez D, Sly PD, Olin AC. Exhaled breath malondialdehyde as a marker of effect of exposure to air pollution in children with asthma. J Allergy Clin Immunol. 2008;121(4):903–9. e906.
25. Gomersall AC, Phan HA, Iacuone S, Li SF, Parish RW. The *Mycoplasma hyorhinis* p37 Protein Rapidly Induces Genes in Fibroblasts Associated with Inflammation and Cancer. PLoS One. 2015;10(10):e0140753.
26. Majumder S, Zappulla F, Silbart LK. *Mycoplasma gallisepticum* lipid associated membrane proteins up-regulate inflammatory genes in chicken tracheal epithelial cells via TLR-2 ligation through an NF-kappaB dependent pathway. PLoS One. 2014;9(11):e112796.
27. Xue D, Ma Y, Li M, Li Y, Luo H, Liu X, Wang Y. *Mycoplasma ovipneumoniae* induces inflammatory response in sheep airway epithelial cells via a MyD88-dependent TLR signaling pathway. Vet Immunol Immunopathol. 2015;163(1–2):57–66.
28. Thannickal VJ, Fanburg BL. Reactive oxygen species in cell signaling. Am J Physiol Lung Cell Mol Physiol. 2000;279(6):L1005–1028.
29. Halliwell B, Whiteman M. Measuring reactive species and oxidative damage in vivo and in cell culture: how should you do it and what do the results mean? Br J Pharmacol. 2004;142(2):231–55.
30. Lee KE, Kim KW, Hong JY, Kim KE, Sohn MH. Modulation of IL-8 boosted by *Mycoplasma pneumoniae* lysate in human airway epithelial cells. J Clin Immunol. 2013;33(6):1117–25.
31. You X, Wu Y, Zeng Y, Deng Z, Qiu H, Yu M. *Mycoplasma genitalium*-derived lipid-associated membrane proteins induce activation of MAPKs, NF-kappaB and AP-1 in THP-1 cells. FEMS Immunol Med Microbiol. 2008;52(2):228–36.
32. Cobb MH. MAP kinase pathways. Prog Biophys Mol Biol. 1999;71(3–4):479–500.
33. Whitmarsh AJ, Davis RJ. Transcription factor AP-1 regulation by mitogen-activated protein kinase signal transduction pathways. J Mol Med (Berl). 1996;74(10):589–607.
34. Ramos JW. The regulation of extracellular signal-regulated kinase (ERK) in mammalian cells. Int J Biochem Cell Biol. 2008;40(12):2707–19.
35. Whelchel A, Evans J, Posada J. Inhibition of ERK activation attenuates endothelin-stimulated airway smooth muscle cell proliferation. Am J Respir Cell Mol Biol. 1997;16(5):589–96.
36. Wesley UV, Bove PF, Hristova M, McCarthy S, van der Vliet A. Airway epithelial cell migration and wound repair by ATP-mediated activation of dual oxidase 1. J Biol Chem. 2007;282(5):3213–20.
37. Bae CH, Kim JS, Song SY, Kim YW, Park SY, Kim YD. Insulin-like growth factor-1 induces MUC8 and MUC5B expression via ERK1 and p38 MAPK in human airway epithelial cells. Biochem Biophys Res Commun. 2013;430(2):683–8.
38. Arnoult D, Parone P, Martinou JC, Antonsson B, Estaquier J, Ameisen JC. Mitochondrial release of apoptosis-inducing factor occurs downstream of cytochrome c release in response to several proapoptotic stimuli. J Cell Biol. 2002;159(6):923–9.
39. Garrido C, Galluzzi L, Brunet M, Puig PE, Didelot C, Kroemer G. Mechanisms of cytochrome c release from mitochondria. Cell Death Differ. 2006;13(9):1423–33.
40. Slee EA, Harte MT, Kluck RM, Wolf BB, Casiano CA, Newmeyer DD, Wang HG, Reed JC, Nicholson DW, Alnemri ES, et al. Ordering the cytochrome c-initiated caspase cascade: hierarchical activation of caspases-2, −3, −6, −7, −8, and −10 in a caspase-9-dependent manner. J Cell Biol. 1999;144(2):281–92.
41. Goldsmith KC, Gross M, Peirce S, Luyindula D, Liu X, Vu A, Sliozberg M, Guo R, Zhao H, Reynolds CP, et al. Mitochondrial Bcl-2 family dynamics define therapy response and resistance in neuroblastoma. Cancer Res. 2012;72(10):2565–77.
42. Brunelle JK, Letai A. Control of mitochondrial apoptosis by the Bcl-2 family. J Cell Sci. 2009;122(Pt 4):437–41.
43. Larbi A, Douziech N, Fortin C, Linteau A, Dupuis G, Fulop Jr T. The role of the MAPK pathway alterations in GM-CSF modulated human neutrophil apoptosis with aging. Immun Ageing. 2005;2(1):6.
44. Boucher MJ, Morisset J, Vachon PH, Reed JC, Laine J, Rivard N. MEK/ERK signaling pathway regulates the expression of Bcl-2, Bcl-X(L), and Mcl-1 and promotes survival of human pancreatic cancer cells. J Cell Biochem. 2000;79(3):355–69.
45. Parhamifar L, Andersen H, Moghimi SM. Lactate dehydrogenase assay for assessment of polycation cytotoxicity. Methods Mol Biol. 2013;948:13–22.
46. Lizard G, Fournel S, Genestier L, Dhedin N, Chaput C, Flacher M, Mutin M, Panaye G, Revillard JP. Kinetics of plasma membrane and mitochondrial alterations in cells undergoing apoptosis. Cytometry. 1995;21(3):275–83.
47. Zelko IN, Mariani TJ, Folz RJ. Superoxide dismutase multigene family: a comparison of the CuZn-SOD (SOD1), Mn-SOD (SOD2), and EC-SOD (SOD3) gene structures, evolution, and expression. Free Radic Biol Med. 2002;33(3):337–49.
48. Green J, Rolfe MD, Smith LJ. Transcriptional regulation of bacterial virulence gene expression by molecular oxygen and nitric oxide. Virulence. 2014;5(8):794–809.
49. Mendez-Samperio P, Perez A, Alba L. Reactive oxygen species-activated p38/ERK 1/2 MAPK signaling pathway in the *Mycobacterium bovis* bacillus Calmette Guerin (BCG)-induced CCL2 secretion in human monocytic cell line THP-1. Arch Med Res. 2010;41(8):579–85.
50. Liu X, Driskell RR, Engelhardt JF. Stem cells in the lung. Methods Enzymol. 2006;419:285–321.
51. Xu X, Liu T, Zhang A, Huo X, Luo Q, Chen Z, Yu L, Li Q, Liu L, Lun ZR, et al. Reactive oxygen species-triggered trophoblast apoptosis is initiated by endoplasmic reticulum stress via activation of caspase-12, CHOP, and the JNK pathway in *Toxoplasma gondii* infection in mice. Infect Immun. 2012;80(6):2121–32.
52. Kumari A, Kakkar P. Lupeol prevents acetaminophen-induced in vivo hepatotoxicity by altering the Bax/Bcl-2 and oxidative stress-mediated mitochondrial signaling cascade. Life Sci. 2012;90(15–16):561–70.
53. Laulier C, Lopez BS. The secret life of Bcl-2: apoptosis-independent inhibition of DNA repair by Bcl-2 family members. Mutat Res. 2012;751(2):247–57.
54. Zuo Y, Xiang B, Yang J, Sun X, Wang Y, Cang H, Yi J. Oxidative modification of caspase-9 facilitates its activation via disulfide-mediated interaction with Apaf-1. Cell Res. 2009;19(4):449–57.
55. Ferrarini MG, Siqueira FM, Mucha SG, Palama TL, Jobard E, Elena-Herrmann B, Vasconcelos AT R, Tardy F, Schrank IS, Zaha A, et al. Insights on the virulence of swine respiratory tract mycoplasmas through genome-scale metabolic modeling. BMC Genomics. 2016;17(1):353.
56. Yang F, Tang C, Wang Y, Zhang H, Yue H. Genome sequence of *Mycoplasma ovipneumoniae* strain SC01. J Bacteriol. 2011;193(18):5018.
57. Rudel T, Kepp O, Kozjak-Pavlovic V. Interactions between bacterial pathogens and mitochondrial cell death pathways. Nat Rev Microbiol. 2010;8(10):693–705.
58. Jones GE, Foggie A, Mould DL, Livitt S. The comparison and characterisation of glycolytic mycoplasmas isolated from the respiratory tract of sheep. J Med Microbiol. 1976;9(1):39–52.

59. Purcell RH, Taylor-Robinson D, Wong D, Chanock RM. Color test for the measurement of antibody to T-strain mycoplasmas. J Bacteriol. 1966;92(1):6–12.
60. Stemke GW, Robertson JA. Comparison of two methods for enumeration of mycoplasmas. J Clin Microbiol. 1982;16(5):959–61.
61. Shen Q, Li C, Feng Q, Sun Y, Ning Y, Zhu L, Wang F. Accurate titration of mycoplasma culture measured by 50% color change unit assay. Wei Sheng Wu Xue Bao. 2013;53(12):1347–52.
62. Winterbourn CC, Buss IH. Protein carbonyl measurement by enzyme-linked immunosorbent assay. Methods Enzymol. 1999;300:106–11.